CHRONOPOTENTIOMETRY WITH AN ALTERNATING CURRENT AT CYLINDRICAL MICROELECTRODES

Angela MOLINA[1], Ricardo RUIZ, Francisco MARTINEZ-ORTIZ[2] and Manuela LOPEZ-TENES[3]

Departamento de Quimica Fisica, Universidad de Murcia, E-30100 Murcia, Spain; e-mail: [1] amolina@fcu.um.es, [2] fmortiz@fcu.um.es, [3] manuela@fcu.um.es

Received April 12, 1995
Accepted January 23, 1996

A theoretical study on the application of the first cycle of alternating current to cylindrical microelectrodes is presented. The analytical expressions obtained here are applicable to electrodes with radii of up to 50 μm, which are in the range of "large" microelectrodes. A method for determination of the kinetic parameter k_s independently of α and methods for calculation of E^0 are proposed.
Key words: Chronopotentiometry; Alternating current; Cylindrical microelectrodes.

In recent papers we have discussed the advantages of the application of a low frequency alternating current to planar and spherical electrodes. Similarly, as in current reversal chronopotentiometry, both the direct and the inverse charge transfer processes[1,2] can be studied simultaneously. However, in relation to current reversal chronopotentiometry, there are two additional advantages:

From a practical point of view, the effect of the charge current is diminished using sinusoidal current compared to constant current. This is due to the fact that the potential–time curves obtained in the first case are less steep both at the beginning of the chronopotentiogram and at the change of the current sign.

From a theoretical point of view, given the continuity with time of the sine function, the mathematical solution of this problem is simpler than in the case of two successive current steps.

In this work we extend the discussion to the case of cylindrical electrodes which have been employed extensively because of their simple fabrication. The first studies in chronopotentiometry at cylindrical electrodes were carried out by Rius et al.[3] who established the theoretical principles from which Peters and Lingane derived their equation for the transition time in constant current chronopotentiometry[4]. Later studies on this subject have been extended to the theory of small radius electrodes but, as far as we know, only current step and some power of time perturbations have been considered[5–8].

In this paper we describe the theory of chronopotentiometry with alternating currents $I(t) = I_0 \sin(wt)$ and $I(t) = I_0 \cos(wt)$ at cylindrical electrodes. We have derived general

equations for transition times of oxidized and reduced species and for potential–time curves. From these expressions we deduce, as particular cases, expressions for stationary planar electrodes and also for the application of a current step. These equations are coincident with those in literature[1,7].

In order to evaluate the range of applicability of our equations, we have studied simultaneously the behaviour of the surface concentrations of species involved in the charge transfer reaction by digital simulation[9]. From our results we conclude that the analytical expressions are applicable to electrodes with radii of up to 50 μm, which are in the range of "large" microelectrodes[10].

Finally, particular features of the potential–time and current–potential curves are discussed. We also propose methods for the calculation of kinetic and thermodynamic parameters of the charge transfer reactions. The calculation is simplified for electrodes with small radii since the magnitude of the capacity component of the current is reduced[11] with respect to its faradaic component.

THEORETICAL

Let us consider the charge transfer reaction

$$\mathrm{A} + n\,\mathrm{e} \underset{k_\mathrm{b}}{\overset{k_\mathrm{f}}{\rightleftharpoons}} \mathrm{B} \quad . \tag{A}$$

When an alternating current $I_\mathrm{j}(t)$ (j can be either s or c) of the form

$$I_\mathrm{s}(t) = I_0 \sin(wt) \tag{1}$$

$$I_\mathrm{c}(t) = I_0 \cos(wt) \tag{2}$$

is applied to a cylindrical electrode, the following initial and boundary conditions are valid

$$\hat{D}_\mathrm{A} C_\mathrm{A} = \hat{D}_\mathrm{B} C_\mathrm{B} = 0 \tag{3}$$

$$\left.\begin{array}{l} t = 0\,, \quad r \geq r_0 \\ t > 0\,, \quad r \to \infty \end{array}\right\} \quad C_\mathrm{A} = C_\mathrm{A}^*\,, \quad C_\mathrm{B} = C_\mathrm{B}^* \tag{4}$$

$t > 0$, $r = r_0$:

$$D_A \left(\frac{\partial C_A}{\partial r} \right)_{r=r_0} = -D_B \left(\frac{\partial C_B}{\partial r} \right)_{r=r_0} = \frac{I_j(t)}{nFA} \tag{5}$$

$$\frac{I_j(t)}{nFA} = k_f C_A(r_0,t) - k_b C_B(r_0,t) \ , \tag{6}$$

where the cylindrical diffusion operator is given by

$$\hat{D}_i = \frac{\partial}{\partial t} - D_i \left(\frac{\partial^2}{\partial r^2} + \frac{1}{r} \frac{\partial}{\partial r} \right) . \tag{7}$$

By using the dimensionless parameters method[12], we obtain the following expressions for the surface concentrations of species A and B

$$\frac{C_A(r_0,t)}{C_A^*} = 1 - N_A t^{1/2} Q_j(\xi_A,\Omega) \tag{8}$$

$$\frac{C_B(r_0,t)}{C_A^*} = \mu + \gamma N_A t^{1/2} Q_j(\xi_B,\Omega) \ , \tag{9}$$

where

$$N_A = \frac{2I_0}{nFAD_A^{1/2} C_A^*} \tag{10}$$

$$\xi_i = \frac{2(D_i t)^{1/2}}{r_0} \tag{11}$$

$$\Omega = wt \tag{12}$$

$$\mu = C_B^*/C_A^* \tag{13}$$

$$\gamma = \left(\frac{D_A}{D_B} \right)^{1/2} \tag{14}$$

and $Q_j(\xi_i,\Omega)$ (i can be either A or B) is a functional series which has the form

$$Q_s(\xi_i,\Omega) = \sum_{k=0}^{\infty} \frac{(-1)^k \Omega^{2k+1}}{(2k+1)!} \lambda_s(\xi_i) \qquad (15)$$

$$\lambda_s(\xi_i) = \frac{p_{4k+2}}{2(4k+3)} - \xi_i \frac{1}{4(4k+4)} + \xi_i^2 \frac{3p_{4k+2}}{32(4k+3)\,(4k+5)} -$$

$$-\xi_i^3 \frac{3}{32(4k+4)\,(4k+6)} + \xi_i^4 \frac{63p_{4k+2}}{1\,024(4k+3)\,(4k+5)\,(4k+7)} -$$

$$-\xi_i^5 \frac{27}{256(4k+4)\,(4k+6)\,(4k+8)} + \xi_i^6 \frac{1\,899\,p_{4k+2}}{16\,384(4k+3)\,(4k+5)\,(4k+7)\,(4k+9)} - \ldots \qquad (16)$$

$$Q_c(\xi_i,\Omega) = \sum_{k=0}^{\infty} \frac{(-1)^k \Omega^{2k}}{(2k)!} \lambda_c(\xi_i) \qquad (17)$$

$$\lambda_c(\xi_i) = \frac{p_{4k}}{2(4k+1)} - \xi_i \frac{1}{4(4k+2)} + \xi_i^2 \frac{3p_{4k}}{32(4k+1)\,(4k+3)} -$$

$$-\xi_i^3 \frac{3}{32(4k+2)\,(4k+4)} + \xi_i^4 \frac{63p_{4k}}{1\,024(4k+1)\,(4k+3)\,(4k+5)} -$$

$$-\xi_i^5 \frac{27}{256(4k+2)\,(4k+4)\,(4k+6)} + \xi_i^6 \frac{1\,899p_{4k}}{16\,384(4k+1)\,(4k+3)\,(4k+5)\,(4k+7)} - \ldots \qquad (18)$$

The transition time τ_A of species A can be reached for cathodic values of the alternating current during its first cycle. From Eq. (*8*) for $C_A(r_0,\tau_A) = 0$ we have

$$\tau_A^{1/2} = \frac{1}{N_A Q_j(\xi_{A,\tau_A},\Omega_{\tau_A})} \; . \qquad (19)$$

If the transition time of the oxidized species is reached, the experiment must be stopped. Under these conditions, the use of an alternating current is not substantially different from other current–time functions[1]. However, there are values of N_A or I_0, Eq. (*10*), for which species A remains undepleted at the electrode surface. In this case the transition time τ_B of species B can be obtained after a change of sign of the current as long

as C_B^* is lower than a predetermined value[1,2]. The condition for the transition time τ_B, $C_B(r_0, \tau_B) = 0$, transforms Eq. (*9*) into

$$\tau_B^{1/2} = -\frac{\mu}{\gamma N_A Q_j(\xi_{B,\tau_B}, \Omega_{\tau_B})} \quad , \tag{20}$$

where ξ_{i,τ_i} and Ω_{τ_i} are the values of ξ_i and Ω in Eqs (*19*) and (*20*), respectively, for $t = \tau_i$. From Eq. (*9*) it can be deduced that τ_B is independent of N_A if B is not initially present in solution.

If neither τ_A nor τ_B is reached during the first cycle of the alternating current, the potential–time (E–t) response shows oscillations around E^0. A more detailed discussion on transition times can be found in refs[1,2].

Inserting Eqs (*8*) and (*9*) into Eq. (*6*), we obtain the following expression for the potential–time function

$$\frac{I_j(t)}{I_0} N_A \frac{D_A^{1/2}}{2k_s} e^{\alpha\eta(t)} = 1 - N_A t^{1/2} Q_j(\xi_A, \Omega) - e^{\eta(t)} [\mu + \gamma N_A t^{1/2} Q_j(\xi_B, \Omega)] \quad , \tag{21}$$

where

$$\eta(t) = \frac{nF}{RT} [E(t) - E^0] \quad . \tag{22}$$

For a reversible process ($k_S \to \infty$), Eq. (*21*) becomes

$$E(t) = E^0 + \frac{RT}{nF} \ln \frac{1 - N_A t^{1/2} Q_j(\xi_A, \Omega)}{\mu + \gamma N_A t^{1/2} Q_j(\xi_B, \Omega)} \quad . \tag{23}$$

In the case of a totally irreversible process ($k_s << 1$ cm s^{-1}), there are following two possibilities:

1. For a cathodic current ($I_j(t) > 0$), Eq. (*21*) has the form

$$E(t) = E^0 + \frac{RT}{\alpha nF} \ln (nFAC_A^* k_S) + \frac{RT}{\alpha nF} \ln M_j^{cath} \tag{24}$$

$$M_j^{cath} = \frac{1 - N_A t^{1/2} Q_j(\xi_A, \Omega)}{I_j(t)} \quad . \tag{25}$$

2. For an anodic current ($I_j(t) < 0$), Eq. (*21*) is simplified to

$$E(t) = E^0 - \frac{RT}{(1-\alpha)nF} \ln (nFAC_A^* k_s) + \frac{RT}{(1-\alpha)nF} \ln M_j^{anod} \qquad (26)$$

$$M_j^{anod} = \frac{-I_j(t)}{\mu + \gamma N_A t^{1/2} Q_j(\xi_B, \Omega)} \ . \qquad (27)$$

Special Cases

Planar Electrode

The equations obtained for a cylindrical electrode can be transformed into those corresponding to a planar electrode by setting $\xi_i = 0$ ($r_0 \to \infty$, Eq. (*11*)) in expressions (*8*), (*9*) and (*21*). Then Eqs (*15*) and (*17*) can be simplified to

$$Q_{s,p}(\Omega) = \sum_{k=0}^{\infty} \frac{(-1)^k \Omega^{2k+1}}{(2k+1)!\, p_{4k+3}} \qquad (28)$$

$$Q_{c,p}(\Omega) = \sum_{k=0}^{\infty} \frac{(-1)^k \Omega^{2k}}{(2k)!\, p_{4k+1}} \ . \qquad (29)$$

Constant Current

Equations corresponding to this case can be obtained by setting $k = 0$ in the series $Q_c(\xi_i, \Omega)$. Thus, Eq. (*17*) is simplified to the form which is in agreement with refs[3–7].

$$Q_c(\xi_i) = \lambda_c(\xi_i) = \frac{1}{\pi^{1/2}} - \frac{1}{8}\xi_i + \frac{1}{16\pi^{1/2}}\xi_i^2 - \frac{3}{256}\xi_i^3 +$$

$$+ \frac{21}{2\,560\pi^{1/2}}\xi_i^4 - \frac{9}{4\,096}\xi_i^5 + \frac{633}{286\,720\pi^{1/2}}\xi_i^6 - \dots \ . \qquad (30)$$

RESULTS AND DISCUSSION

In order to establish the validity range of $Q_j(\xi_i, \Omega)$ in Eqs (*15*) and (*17*), we have carried out a parallel study of process (*A*) using digital simulation by the Crank–Nicolson

method with the implicit calculation of boundary values (surface concentration)[9]. In Fig. 1 the dependence of the surface concentration of B on ξ_B is shown for different angular frequencies *w*, obtained from Eq. (*9*) and by digital simulation. Both procedures are in a very good agreement under the conditions of Fig. 1. For alternating current with amplitude I_0, this agreement improves with decreasing *w* (Eq. (*1*), Fig. 1a) and with increasing *w* for an alternating current given by Eq. (*2*), Fig. 1b. From these plots it is evident that in the case of chronopotentiometry with alternating current our equations are valid for "large" microelectrodes. Indeed, the maximum time of the experiment is closely related to the electrode radius by Eq. (*11*). Therefore, for $D_i = 10^{-5}$ cm^2 s^{-1} if the time does not exceed 2.5 s, the radius of the electrode can have a value of 0.005 cm ($\xi_i = 2$). Obviously, the radius can be smaller if the electrolysis time decreases.

In Fig. 2 we have plotted the *E*–*t* curves for a reversible process and several values of N_A when there is a transition time for species B and a small cylindrical electrode of 0.005 cm radius is used. These curves intersect at the point corresponding to the potential E_R defined by Eq. (*31*) for $D_A = D_B$ ($\gamma = 1$) (see Eq. (*23*) with $Q_j(\xi_i,\Omega) = 0$)

$$E_R = E^0 + \frac{RT}{nF} \ln \frac{1}{\mu} \quad . \tag{31}$$

This type of plot can be used to estimate E^0 from Eq. (*31*). In the case of planar electrodes, the point of intersection exists even at $\gamma \neq 1$. Obviously, E_R is defined only if species B is initially present in solution.

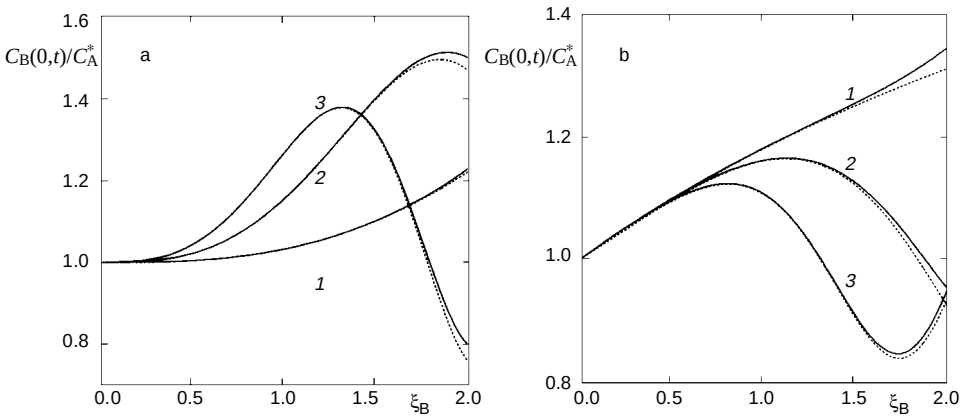

FIG. 1

Variation of surface concentration of species B with parameter ξ_B obtained from Eq. (*9*) (———) and by digital simulation (· · · ·). a The alternating current applied is given by Eq. (*1*); $\gamma = 1$, $D_B = 10^{-5}$ cm^2 s^{-1}, $N_A = 1$ s$^{-1/2}$, $\mu = 1$, $r_0 = 0.005$ cm. The values of *w*: *1* 0.2, *2* 1, *3* 2 s^{-1}. b The alternating current applied is given by Eq. (*2*). $N_A = 0.5$ s$^{-1/2}$. The values of *w*: *1* 0 (current step), *2* 1, *3* 2 s^{-1}. Other conditions as in 1a

Figure 3 corresponds to a process with $k_s = 10^{-4}$ cm s^{-1}. We have plotted the chronopotentiograms for three values of α for a small cylindrical electrode of 0.007 cm radius and for the species B initially absent in the solution (μ = 0). In this case we can observe other points of intersection:

The point III corresponds to the values of t_c and E_c on coordinates. Here t_c is the time at which the alternating current I_j (t_c) = 0, and E_c is the zero-current potential which does not depend on the kinetic parameters of the process[13]. It can be derived from Eqs (*21*) or (*23*) in the form

$$E_c = E^0 + \frac{RT}{nF} \ln \frac{1 - N_A t_c^{1/2} Q_j(\xi_{A,t_c}, \Omega_{t_c})}{\mu + \gamma N_A t_c^{1/2} Q_j(\xi_{B,t_c}, \Omega_{t_c})} \quad , \qquad (32)$$

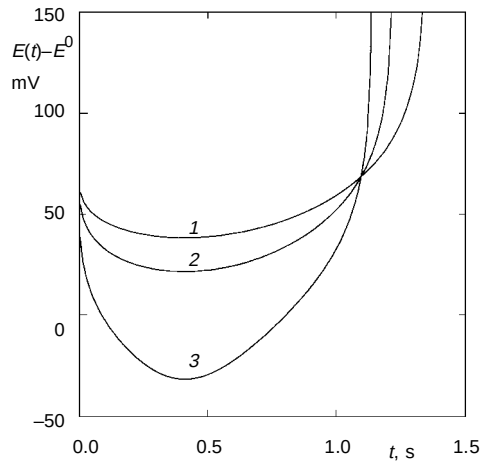

FIG. 2
Potential–time (*E*–*t*), plot for a reversible process (Eq. (*23*)). The alternating current applied is given by Eq. (*2*). T = 298 K, n = 1, $D_A = D_B = 10^{-5}$ cm^2 s^{-1}, w = 2 s^{-1}, μ = 0.07, r_0 = 0.005 cm. The values of N_A: *1* 0.5, *2* 1, *3* 3 s$^{-1/2}$

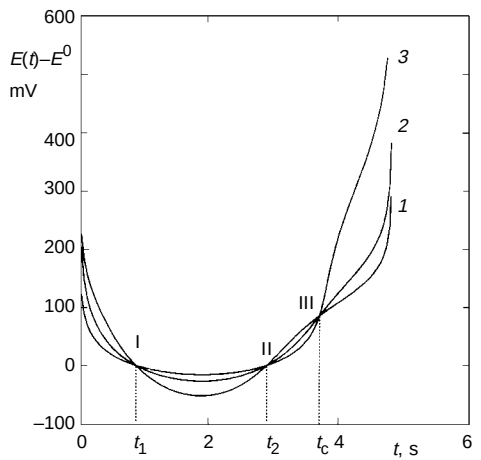

FIG. 3
Influence of α on *E*–*t* curves for $k_s = 10^{-4}$ cm s^{-1} (Eq. (*21*)). The alternating current applied is given by Eq. (*1*), $D_A = 8 \cdot 10^{-6}$ cm^2 s^{-1}, $D_B = 10^{-5}$ cm^2 s^{-1}, w = 0.85 s^{-1}, N_A = 0.1 s$^{-1/2}$, μ = 0, r_0 = 0.007 cm. The values of α: *1* 0.2, *2* 0.4, *3* 0.7. Other conditions are the same as in Fig. 2, description of t_1, t_2, t_c and I–III in text

where ξ_{i,t_c} and Ω_{tc} are the values of the parameters ξ_i and Ω for $t = t_c$. Figure 3 presents two other points of intersection (at t_1 and at t_2). In both cases $E(t_1) = E(t_2) = E^0$. Values of t_1 and t_2 have the advantage of being independent of α, but they depend on k_s as follows from Eqs (*21*) and (*22*).

With respect to this feature, it is convenient to construct curves such as those shown in Fig. 4, where we present the variation of t_1 (curves *I*) and t_2 (curves *II*) with log k_s for several values of N_A. Therefore, from points III, I and/or II it is possible to determine the values of E^0 and k_s. For a specific chronopotentiogram we can proceed in three steps.

1. As the time t_c corresponding to a zero current is obtained from Eq. (*1*) or (*2*), the corresponding E_c value can be measured and, from Eq. (*32*), the value of E^0 can be obtained.

2. Once E^0 is known, curves of the type shown in Fig. 4 can be used to estimate the value of k_s. One can obtain values of k_s for a wide range of this experimental variable simply by changing the experimental conditions.

3. After E^0 and k_s were determined, the value of α at any point of the curve can be obtained from Eq. (*21*).

For a totally irreversible process, the *E*–*t* response is noticeably simplified (Eqs (*24*) and (*26*)). In this case parameters α, k_s and E^0 can be obtained by plotting $E(t)$ against ln M_j^{cath} and $E(t)$ against ln M_j^{anod}, refs[1,2].

Figure 5 shows effects exerted by an initial concentration of species B, through the parameter $\mu = C_B^*/C_A^*$, on the *E*–*t* curves plotted for $k_s = 5 \cdot 10^{-5}$ cm s^{-1} (*1*) and $k_s = 2 \cdot 10^{-6}$ cm s^{-1} (*2*). From curves (*I*) we notice that τ_B exists when $\mu = 0$. There is no transition time either for species A or species B if $\mu = 1$, curves (*II*). In this case, $\mu > \mu_{lim}$ (refs[1,2]). Also, the cathodic branch of the curves becomes independent of μ with decreasing k_s as corresponds to a totally irreversible process in agreement with Eq. (*24*).

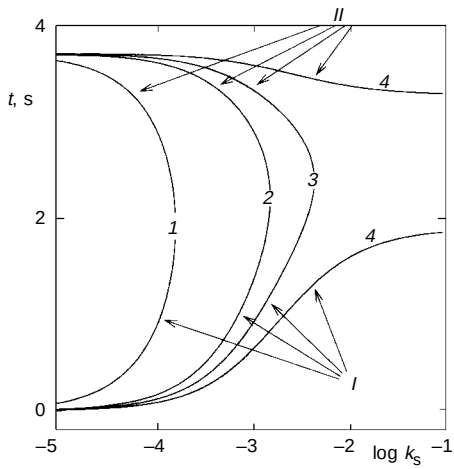

FIG. 4
Variation of $t = t_1$, curves *I* and $t = t_2$, curves *II* with log k_s (in cm s^{-1}), $D_A = 10^{-5}$ cm^2 s^{-1}, $\alpha = 0.5$. The values of N_A: *1* 0.1, *2* 0.5, *3* 0.7, *4* 1 s$^{-1/2}$. Other conditions as in Fig. 3

Figure 6 shows the $i(t)$–$E(t)$ plot, where $i(t) = I_j(t)/I_0$, for a complete cycle of the sine function (when τ_B does not exist) for various values of k_s. The zero-current potential E_c corresponds to the intercept of the right-hand branch of each curve with the zero-current line. The value of kinetic parameters can be obtained from the difference between the potential E_M corresponding to i_{max} and the potential E_m corresponding to i_{min} where

$$i_{max} = 1 \qquad \text{for } t_M = \frac{\pi}{2w} \tag{33}$$

$$i_{min} = -1 \qquad \text{for } t_m = \frac{3\pi}{2w} \tag{34}$$

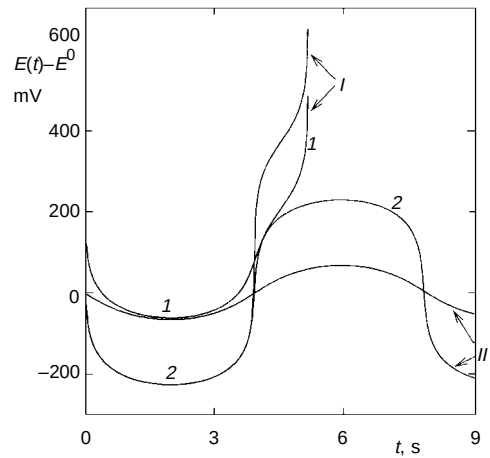

FIG. 5
Dependence of E–t curves on μ, for $k_s = 5 \cdot 10^{-5}$ cm s^{-1} (*1*) and $k_s = 2 \cdot 10^{-6}$ cm s^{-1} (*2*); $D_A = 10^{-5}$ cm^2 s^{-1}, $w = 0.8$ s^{-1}, $r_0 = 0.05$ cm, $\alpha = 0.5$; *I* $\mu = 0$, *II* $\mu = 1$. Other conditions as in Fig. 3

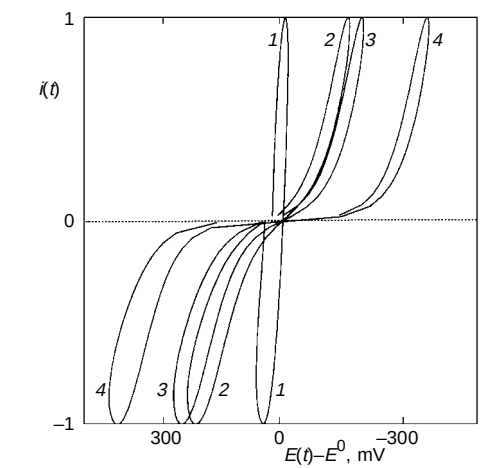

FIG. 6
Influence of k_s on i–E curves according to Eq. (*21*) (no transition time for A and B). $D_A = 10^{-5}$ cm^2 s^{-1}, $w = 2$ s^{-1}, $N_A = 1$ s$^{-1/2}$, $\mu = 0.5$, $r_0 = 0.01$ cm, $\alpha = 0.5$. The values of k_s: *1* $1 \cdot 10^3$, *2* $1 \cdot 10^{-4}$, *3* $5 \cdot 10^{-5}$, *4* $2 \cdot 10^{-6}$ cm s^{-1}. Other conditions as in Fig. 3

$$\Delta E_m^M = E_M - E_m \quad . \tag{35}$$

It is possible to determine α and k_s from ΔE_m^M–log k_s plot using a procedure similar to that described in ref.[2].

From Figs 2, 3, 5 and 6 it is apparent that both *E–t* and *i–E* curves are influenced by k_s so significantly that the degree of reversibility of the electrode process can be estimated by means of simple visual inspection.

The authors greatly appreciate the financial support of the Direccion General de Investigacion Científica y Tecnica (Projects No. PB90-0307, PB93-1134) and DREUCA de la region de Murcia (Project No. PIB 94/73).

SYMBOLS

A	area of cylindrical electrode, cm^2
C_i^*	bulk concentration of species i, mol cm^{-3}
D_i	diffusion coefficient of species i, $cm^2\ s^{-1}$
E_c	zero-current potential, V
E^0	formal potential, V
$E(t)$	time-dependent electrode potential, V
$i(t)$	$I_j(t)/I_0$
I_0	amplitude of the alternating current, A
$I_j(t)$	applied alternating current $I_0 \sin(wt)$ for j = s or $I_0 \cos(wt)$ for j = c, A
k_f, k_b	heterogeneous rate constants of the forward (k_f) and the reverse (k_b) charge transfer reaction, cm s^{-1}
k_s	apparent heterogeneous rate constant of charge transfer at E^0, cm s^{-1}
N_A	$2I_0/nFAD_A^{1/2}C_A^*$, $s^{-1/2}$
p_x	$2\Gamma(1 + x/2)/\Gamma((1 + x)/2)$
r	distance from the generatrix of the cylindrical electrode, cm
r_0	electrode radius, cm
t	time elapsed between switching on the alternating current and the measurement of the potential, s
w	angular frequency, s^{-1}
α	electron transfer coefficient
γ	$(D_A/D_B)^{1/2}$
Γ	Euler gamma-function
μ	C_B^*/C_A^*
ξ_i	$2(Dit)^{1/2}/r_0$
τ_A	transition time for reduction process, s
τ_B	transition time for oxidation process, s
Ω	wt

All other symbols have their usual meaning.

REFERENCES

1. Martinez-Ortiz F., Molina A., Serna C.: J. Electroanal. Chem. *308*, 97 (1991).
2. Molina A., Martinez-Ortiz F., Serna C.: J. Electroanal. Chem. *336*, 1 (1992).
3. Rius A., Polo S., Llopis J.: An. Quim. *45*, 1029 (1949).
4. Peters D. G., Lingane J. J.: J. Electroanal. Chem. *2*, 1 (1961).
5. Evans D. H., Price J. E.: J. Electroanal. Chem. *5*, 77 (1963).
6. Dornfeld D. I., Evans D. H.: J. Electroanal. Chem. *20*, 341 (1969); and references therein.
7. Aoki K., Honda K., Tokuda K., Matsuda H.: J. Electroanal. Chem. *195*, 51 (1985).
8. Hurwitz H. D.: J. Electroanal. Chem. *2*, 142 (1961).
9. Britz D.: *Digital Simulation in Electrochemistry*. Springer, Berlin 1988.
10. Pletcher D. in: *Microelectrodes: Theory and Applications* (M. I. Montenegro, M. A. Queiros and J. L. Daschbach, Eds). Kluwer Academic Publishers, The Netherlands 1991.
11. Abrantes L. M., Fleischmann M., Li L. J., Hawkins M., Pons J. W., Daschbach J., Pons S.: J. Electroanal. Chem. *262*, 55 (1989).
12. Koutecky J.: Czech. J. Phys. *2*, 50 (1953).
13. Heyrovsky J., Kuta J.: *Principles of Polarography*, p. 128. Academic Press, New York 1966.